Electronic Supplementary Material (ESI) for Physical Chemistry Chemical Physics.

Supplementary Material

NMR spectroscopic studies of a TAT-derived model peptide in imidazolium-based ILs: influence on chemical shifts and the *cis/trans* equilibrium state

Christoph Wiedemann[1], Oliver Ohlenschäger[2], Carmen Mrestani-Klaus[1], and Frank Bordusa[1,*]

[1] *Institute of Biochemistry and Biotechnology, Martin-Luther-University Halle-Wittenberg, Kurt-Mothes-Str. 3, 06120 Halle, Germany*

[2] *Leibniz Institute on Aging - Fritz Lipmann Institute, Beutenbergstr. 11, 07745 Jena, Germany*

[*] *Corresponding author: frank.bordusa@biochemtech.uni-halle.de*

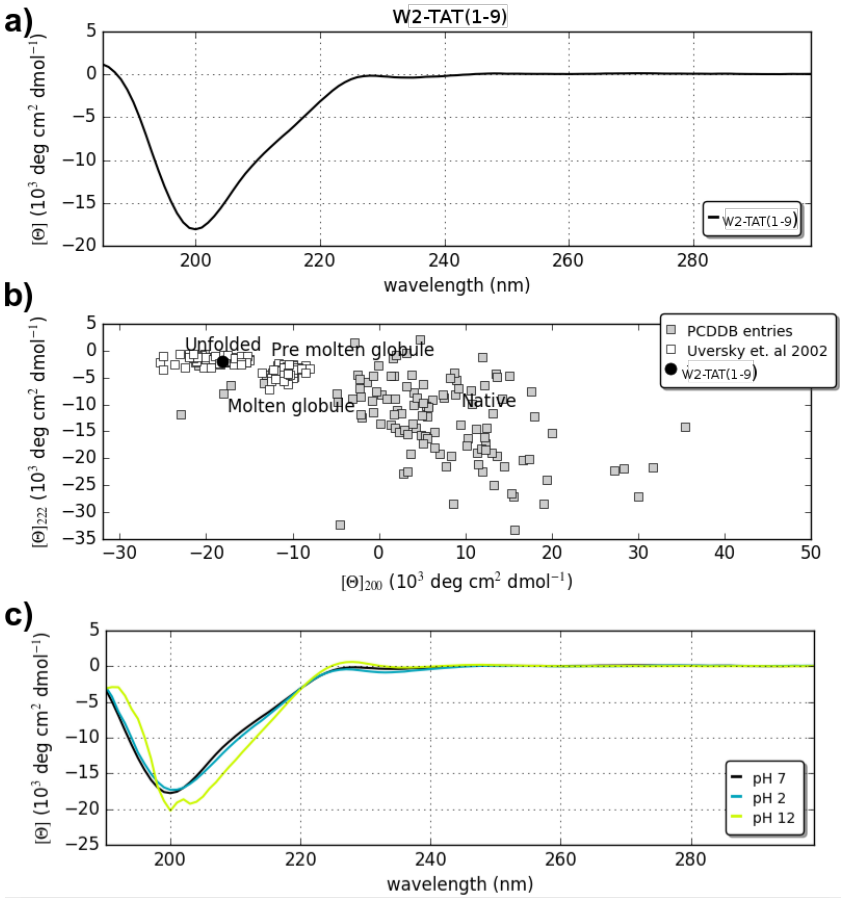

Fig. S 1: a) Far UV-CD spectra of the W2-TAT(1-9) peptide dissolved in water. Circular dichroism (CD) spectra were recorded on a JASCO J-710 CD spectropolarimeter at 303.2 K in a 1 mm quartz cuvette to estimate the secondary structure content. The instrument was calibrated with D-10-camphorsulphonic acid (Sigma Aldrich). The peptide concentration was 157 μM and verified spectrophotometrically at 280 nm with the extinction coefficient calculated using ProtParam (http://web.expasy.org/protparam/). Each CD spectrum represents the average of 3 accumulated scans at 20 nm/ min with a 1 nm slit width and a time constant of 2 s for a nominal resolution of 0.7 nm. Data were collected between 185 and 320 nm by taking points every 1 nm. No further zeroing was applied after background subtraction. Data were processed and visualized with CAPITO [1]. **b)** The 'double wavelength' plot ($[\Theta]_{200}$ plotted versus $[\Theta]_{222}$) allows to deduce the folding state of TAT(W2) [2]. **c)** Far UV-CD spectra of the TAT(W2) collected at pH 7 (black), pH 2 (blue) and pH 12 (green). Experimental conditions as described above.

Table S 1: The secondary structure elements of W2-TAT(1-9) estimated from CD spectrum. Estimation of structural contents are given in percent.

	helical	β-strand	irregular
CAPITO[a]	4–13	18–41	55–69
SELCON3[b]	10	29	61
CONTIN[b]	8	33	59
CDSSTR[b]	6	33	61
DSSP *trans* W2-TAT(1-9)[c]	0	33	67
DSSP *cis* W2-TAT(1-9)[c]	0	55	45

[a] [1]
[b] included in the software CDPro [3]
[c] secondary structure determination based on the ROE calculated structures [4]

Table S 2: ^{1}H, ^{13}C and ^{15}N chemical shift assignments of the *trans* configured W2-TAT(1-9) peptide in aqueous solution (90% H_2O/10% D_2O (v/v), pH 6.5) at 303.2 K

	H	N	N^{δ}	N^{ϵ}	H^{α}	H^{β}	H^{γ}	H^{δ}	H^{ϵ}	H^{ζ}	H^{η}	C	C^{α}	C^{β}	C^{γ}	C^{δ}	C^{ϵ}	C^{ζ}	C^{η}
M1					3.92	2.03,2.03	2.48,2.48		2.02			172.62	55.31	33.18	30.93		16.76		
W2				129.38	5.02	3.15,3.34		7.29	10.13,7.71	7.18,7.51	7.26	174.10	55.14	29.10	111.33	129.47,127.70	120.97,138.89	122.25,114.86	124.83
P3					4.45	2.24,1.89	1.96,1.96	3.78,3.49				176.48	63.31	31.99	27.30	50.86			
V4	8.00	119.83			4.09	2.01	0.92,0.92					175.65	62.05	33.03	20.48,20.48				
D5	8.31	125.63			4.84	2.54,2.79						174.81	52.06	41.54	179.94				
P6					4.41	2.22,1.93	1.95,1.95	3.81,3.81				176.80	63.50	32.19	26.94	50.88			
N7	8.52	118.03	114.08		4.68	2.80,2.75		7.76,6.90				175.08	53.74	38.96	177.29				
I8	7.75	120.40			4.19	1.90	0.90,1.42,1.16	0.86				175.19	61.34	38.97	27.07,17.50	12.98			
E9	7.89	129.76			4.11	1.99,1.88	2.18,2.18					180.92	58.19	31.30	36.67	184.64			

Table S 3: ^{1}H, ^{13}C and ^{15}N chemical shift assignments of the *cis* configured W2-TAT(1-9) peptide in aqueous solution (90% H_2O/10% D_2O (v/v), pH 6.5) at 303.2 K

	H	N	N^{δ}	N^{ϵ}	H^{α}	H^{β}	H^{γ}	H^{δ}	H^{ϵ}	H^{ζ}	H^{η}	C	C^{α}	C^{β}	C^{γ}	C^{δ}	C^{ϵ}	C^{ζ}	C^{η}
M1					4.15	2.16,2.16	2.61,2.61		2.15			171.85	55.29	33.16	30.89		16.81		
W2				130.13	4.58	3.29,3.16		7.27	10.21,7.60	7.17,7.52	7.26	173.88	56.41	30.89	110.89	129.41,127.48	120.86,138.97	122.25,114.86	124.81
P3					3.38	1.60,1.07	1.42,1.47	3.21,3.37				175.62	62.97	33.49	24.36	49.99			
V4	7.83	120.82			3.84	1.99	0.89,0.89					175.77	63.21	32.48	21.07,21.07				
D5	8.02	124.23			4.82	2.74,2.47						174.79	51.96	41.61	179.74				
P6					4.40	2.22,1.95	1.93,1.93	3.77,3.77				176.90	63.50	32.17	26.89	50.84			
N7	8.50	117.99	114.03		4.66	2.80,2.74		7.72,6.89				174.89	53.75	38.97	177.38				
I8	7.80	120.46			4.19	1.90	1.16,1.42,0.88	0.85				175.19	61.32	38.96	27.06,17.46	12.98			
E9	7.88	129.58			4.11	2.00,1.87	2.18,2.18					180.90	58.19	31.30	36.67	184.59			

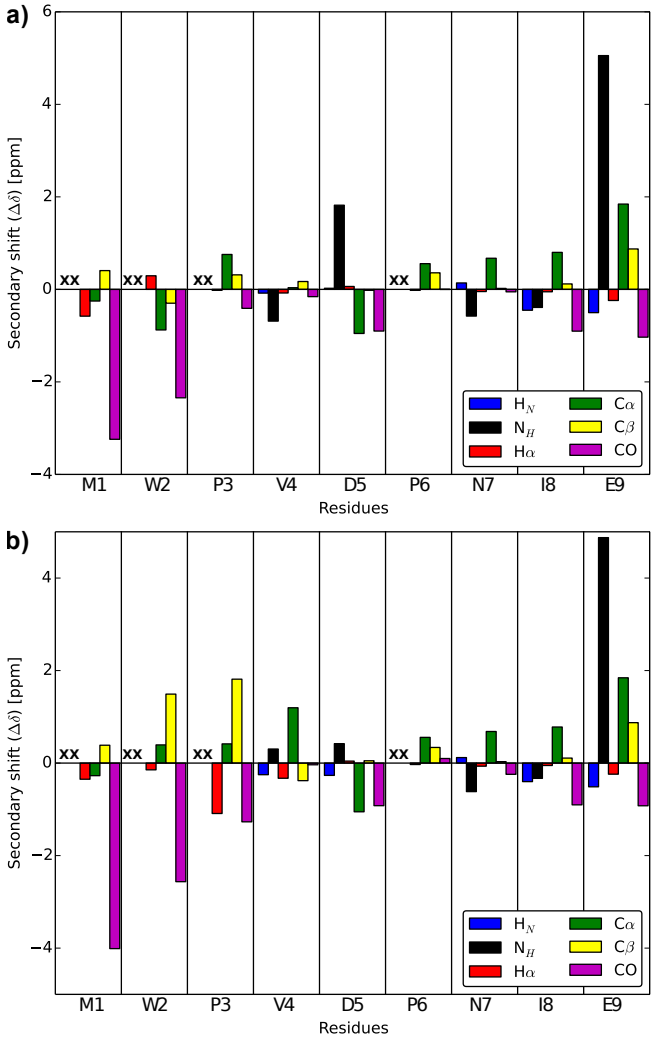

Fig. S 2: Secondary chemical shifts of the W2-TAT(1-9) *all-trans* **(a)** and *cis* **(b)** isoform. Secondary shifts are defined as the difference between the observed chemical shift and the corresponding random coil value. Random coil chemical shifts of the W2-TAT(1-9) peptide were calculated using the CamCoil webserver [5].

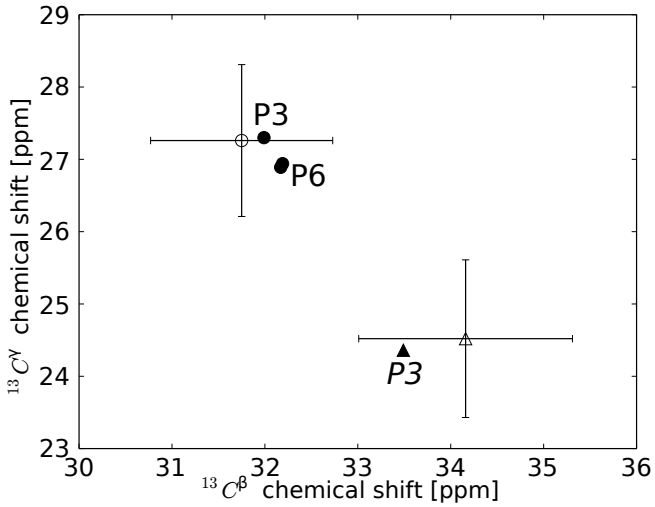

Fig. S 3: Proline $^{13}C^{\beta}$ and $^{13}C^{\gamma}$ chemical shift analysis for the *cis*- and *all-trans*-configured W2-TAT(1-9) peptide. Filled circles and filled triangle correspond to the chemical shifts characteristics of the numbered amino acids. The average $^{13}C^{\beta}$ and $^{13}C^{\gamma}$ chemical shifts for *cis* and *trans* proline is given by open triangle and open circle, respectively [6, 7]. Standrad deviations are indicated by bars.

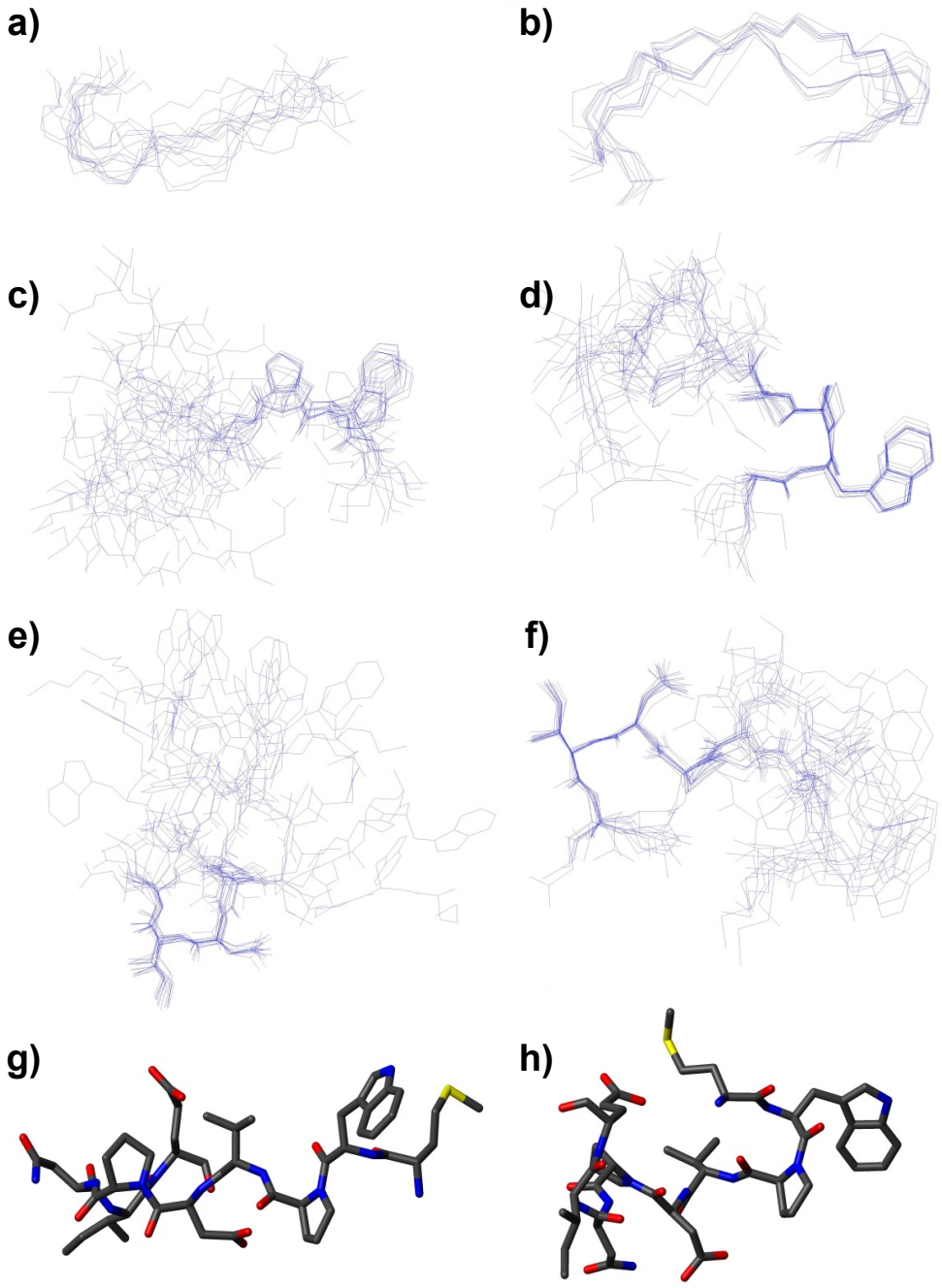

Fig. S 4: NMR solution structures of the *all-trans* **(a,c,e,g)** and *cis* **(b,d,f,h)** isoform of the W2-TAT(1-9) peptide. **(a,b)** Superimposed backbone traces for the 15 structures with the lowest energy after OPAL refinement. In the *all-trans* conformer residues 6-9 superimpose with a backbone r.m.s.d. of 0.58 and resemble a turn-like structure **(e)** whilst the more N-terminal residues are disordered **(c)**. In contrast, in the *cis* conformer the residues M1-V4 **(d)** and P6-E9 **(f)** superimpose with r.m.s.d. values of 0.23 and 0.30 , respectively, indicating the higher structural definition of the cis conformer. Although no standard turn elements could be deduced, in both, the N- and C-terminal stretches these loop elements revert the backbone direction by 180° (*all-trans* **(g)**, *cis* **(h)**).

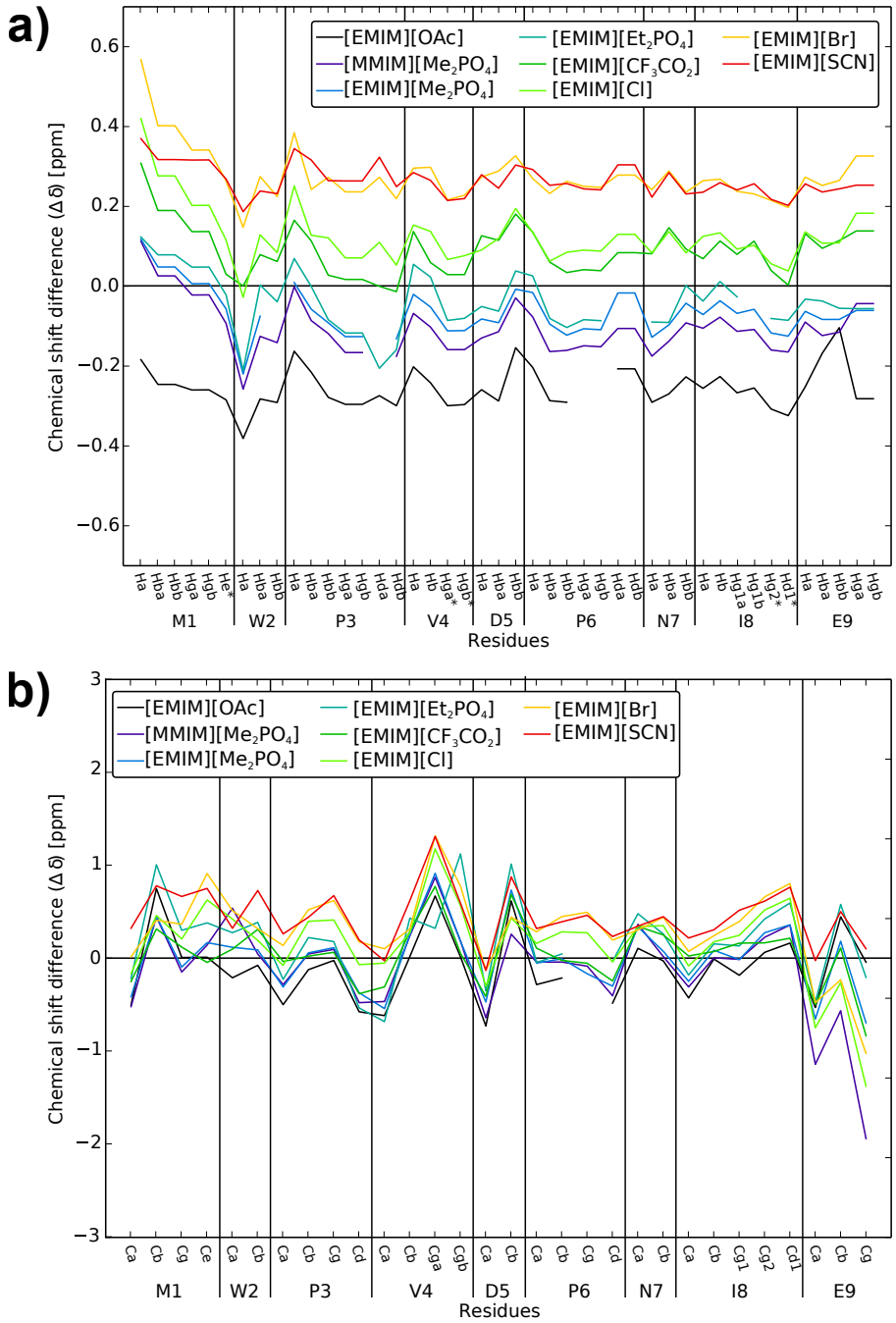

Fig. S 5: ^{1}H **(a)** and ^{13}C **(b)** NMR chemical shift differences ($\Delta\delta$) of *all-trans*-configured W2-TAT(1-9) in various IL/ solvent systems at 303 K. W2-TAT(1-9) concentration in IL/ solvent systems was 90 mM and 10 mM in the reference water system, respectively. The IL concentration was 3 M (approximately 70% IL/30% D_2O v/v). In all experiments pH was adjusted to 6.5.

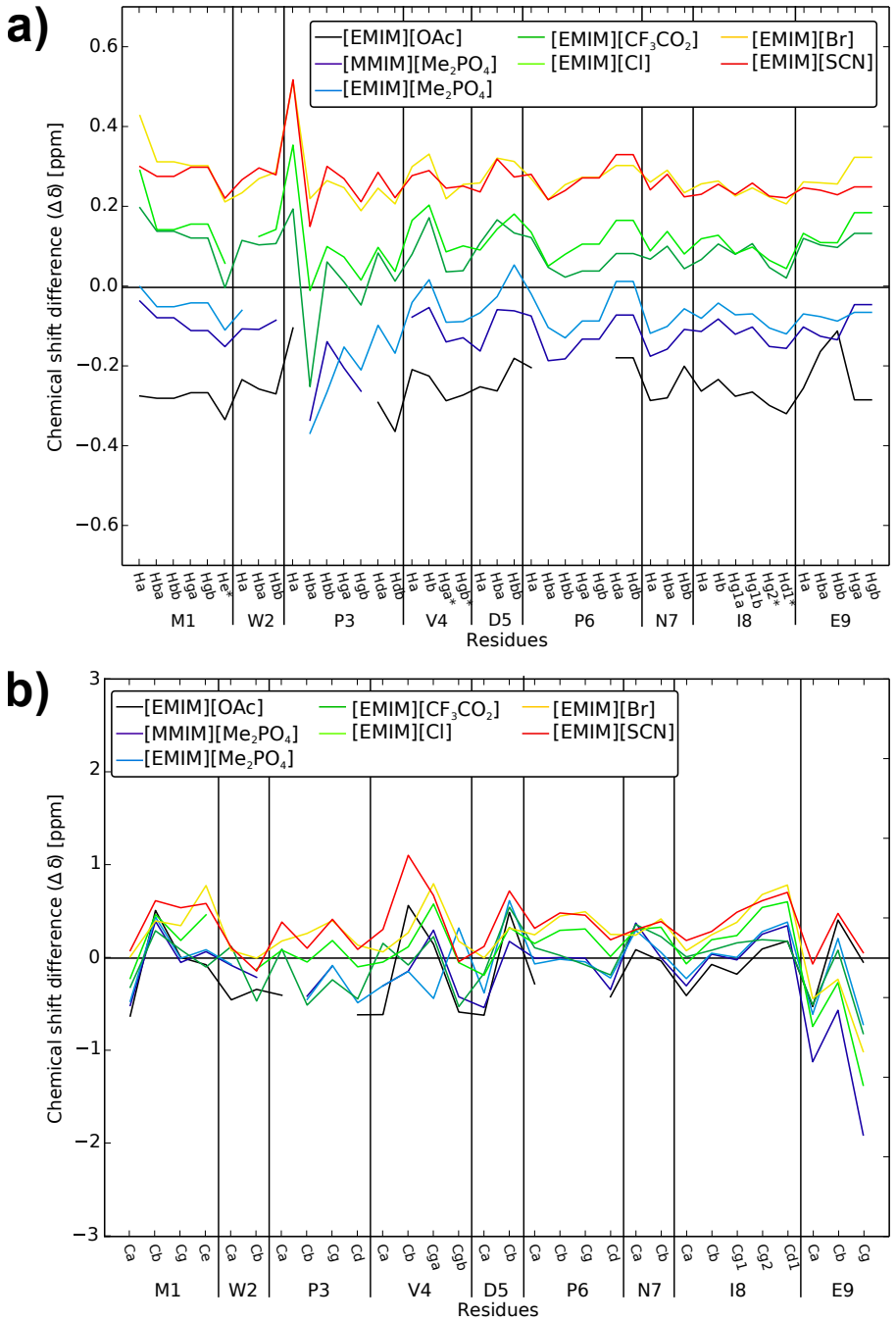

Fig. S 6: ^{1}H **(a)** and ^{13}C **(b)** NMR chemical shift differences ($\Delta\delta$) of *cis*-configured W2-TAT(1-9) in various IL solvent systems at 303 K. W2-TAT(1-9) concentration in IL/ solvent systems was 90 mM and 10 mM in the reference water system, respectively. The IL concentration was 3 M (approximately 70% IL/30% D_2O v/v). In all experiments pH was adjusted to 6.5. The spectral quality of the 3M [EMIM][Et_2PO_4] sample allows only the assignment of a few unambiguous *cis*-configured W2-TAT(1-9) signals.

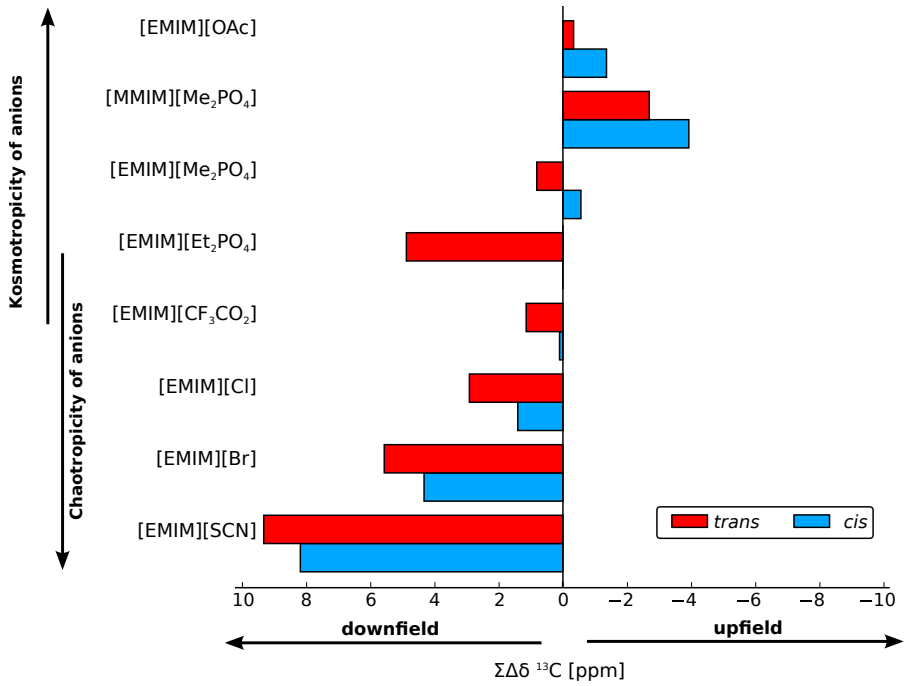

Fig. S 7: Summed up ^{13}C chemical shift differences ($\sum \Delta\delta$) of selected carbons for *cis*-(blue) and *all-trans*-configured (red) W2-TAT(1-9) peptide in different IL solvent systems.

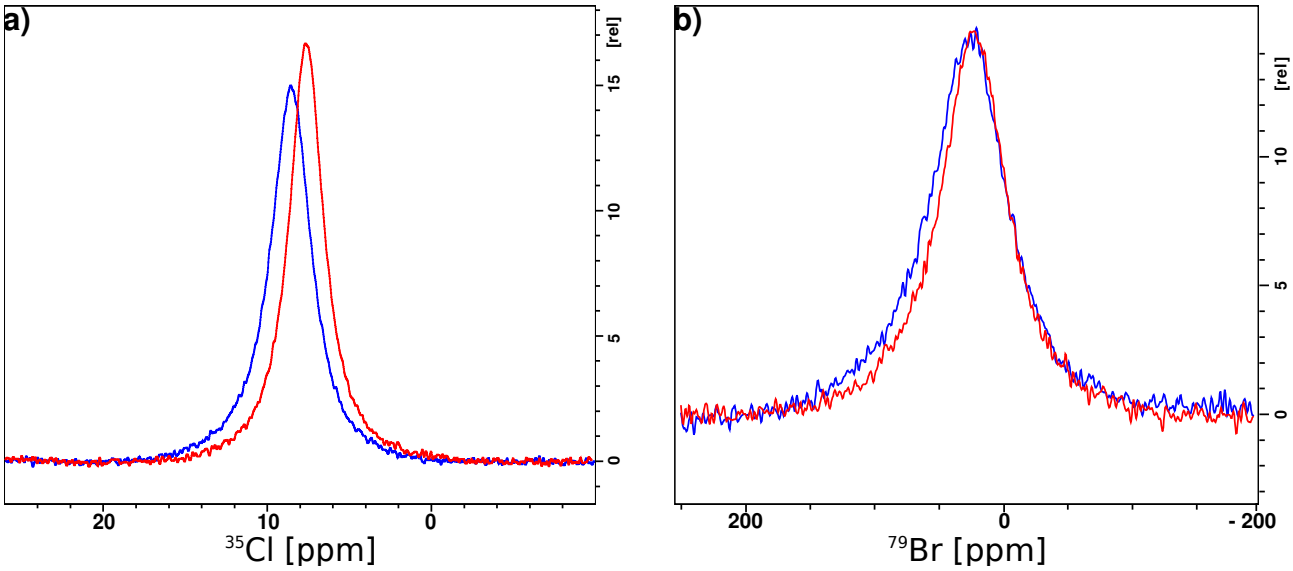

Fig. S 8: a) ^{35}Cl chemical shifts of pure [EMIM][Cl] (7.66 ppm, red line) and in the presence of 10 mM W2-TAT(1-9) peptide (8.56 ppm, blue line). **b)** ^{79}Br chemical shifts of pure [EMIM][Br] (23.6 ppm, red line) and in the presence of 10 mM W2-TAT(1-9) peptide (30.7 ppm, blue line). Spectra were collected at 303 K on a Bruker 400 MHz AvanceIII system equipped with a 5 mm room-temperatue double resonance broad band probe and 32 transients. The probe was tuned to the appropriate frequencies. The spectral width for ^{35}Cl was 2354 Hz with transmitter frequency offset of 0 Hz and acquisition time was 0.217 s with a recycle delay of 1 s. The ^{35}Cl pulse length was 14 μs at 90 W. The spectral width for ^{79}Br was 10 kHz with transmitter frequency offset of 1303.23 Hz and acquisition time was 0.00512s with a recycle delay of 1 s. The ^{79}Br pulse length was 8 μs at 60 W. The ^{35}Cl chemical shifts were referenced to 0.1 M NaCl solution in D_2O. The ^{79}Br chemical shifts were referenced to 0.1 M KBr solution in D_2O.

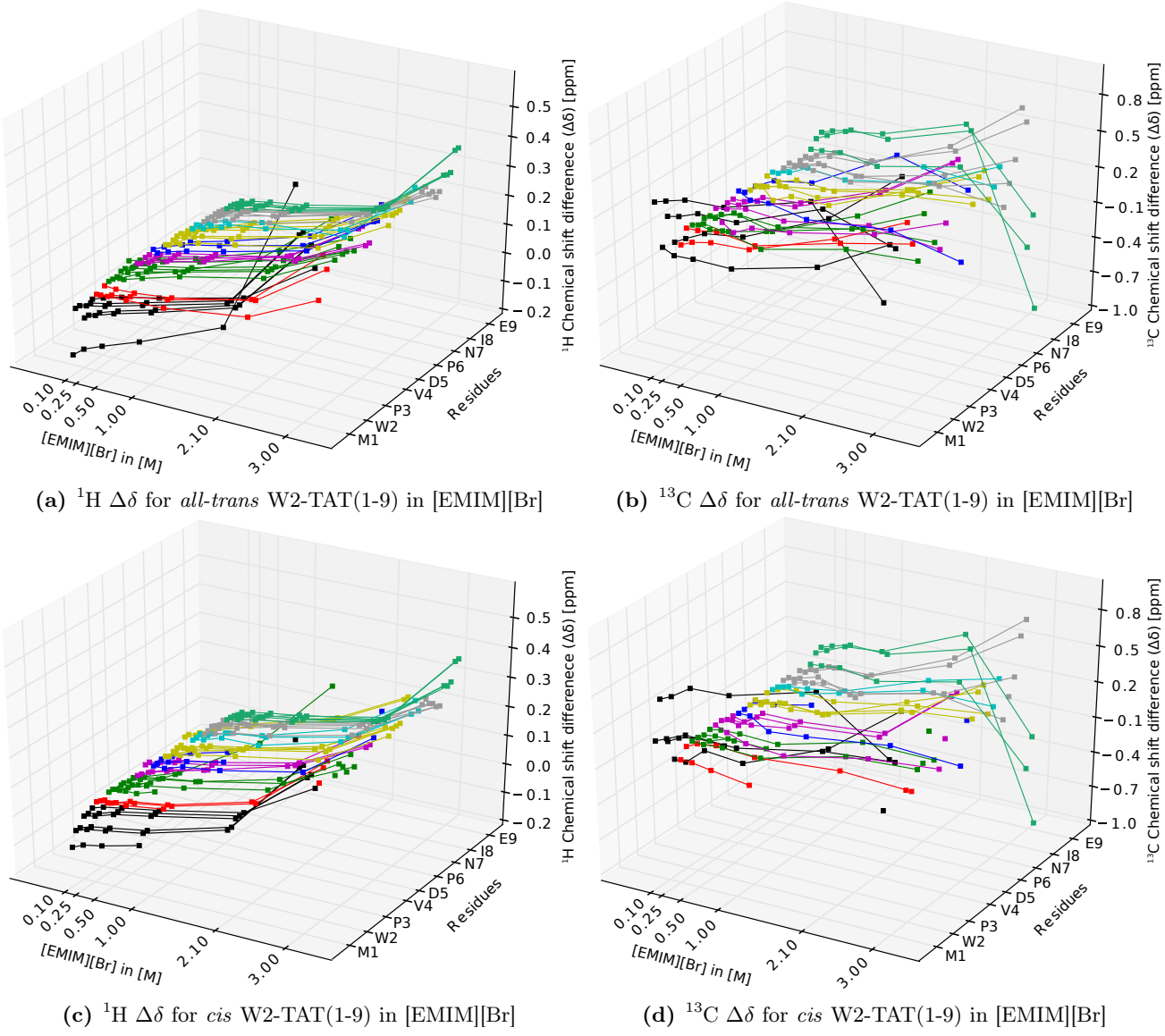

(a) ^{1}H $\Delta\delta$ for *all-trans* W2-TAT(1-9) in [EMIM][Br]

(b) ^{13}C $\Delta\delta$ for *all-trans* W2-TAT(1-9) in [EMIM][Br]

(c) ^{1}H $\Delta\delta$ for *cis* W2-TAT(1-9) in [EMIM][Br]

(d) ^{13}C $\Delta\delta$ for *cis* W2-TAT(1-9) in [EMIM][Br]

Fig. S 9: ^{1}H and ^{13}C chemical shift differences ($\Delta\delta$) of protons and carbons for *all-trans*- (upper panel) and *cis*-configured (lower panel) W2-TAT(1-9) as function of [EMIM][Br] concentration. The reference system was 10 mM W2-TAT(1-9), pH 6.5, in 90/10% H_2O/D_2O. The peptide concentration was 10 mM for samples up to 2.1 M [EMIM][Br] and experiments were carried out with a 5 mm room-temperature BBI-probe. Spectra for 3 M [EMIM][Br] were carried out with a 4 mm triple resonance HR-MAS probe at 6 kHz spinning rate and a W2-TAT(1-9) concentration of 90 mM. All NMR experiments were acquired at 303 K and the pH was adjusted to 6.5. Depicted are all ^{1}H and ^{13}C $\Delta\delta$ in sequential order per residue as given in Fig. S5 and S6.

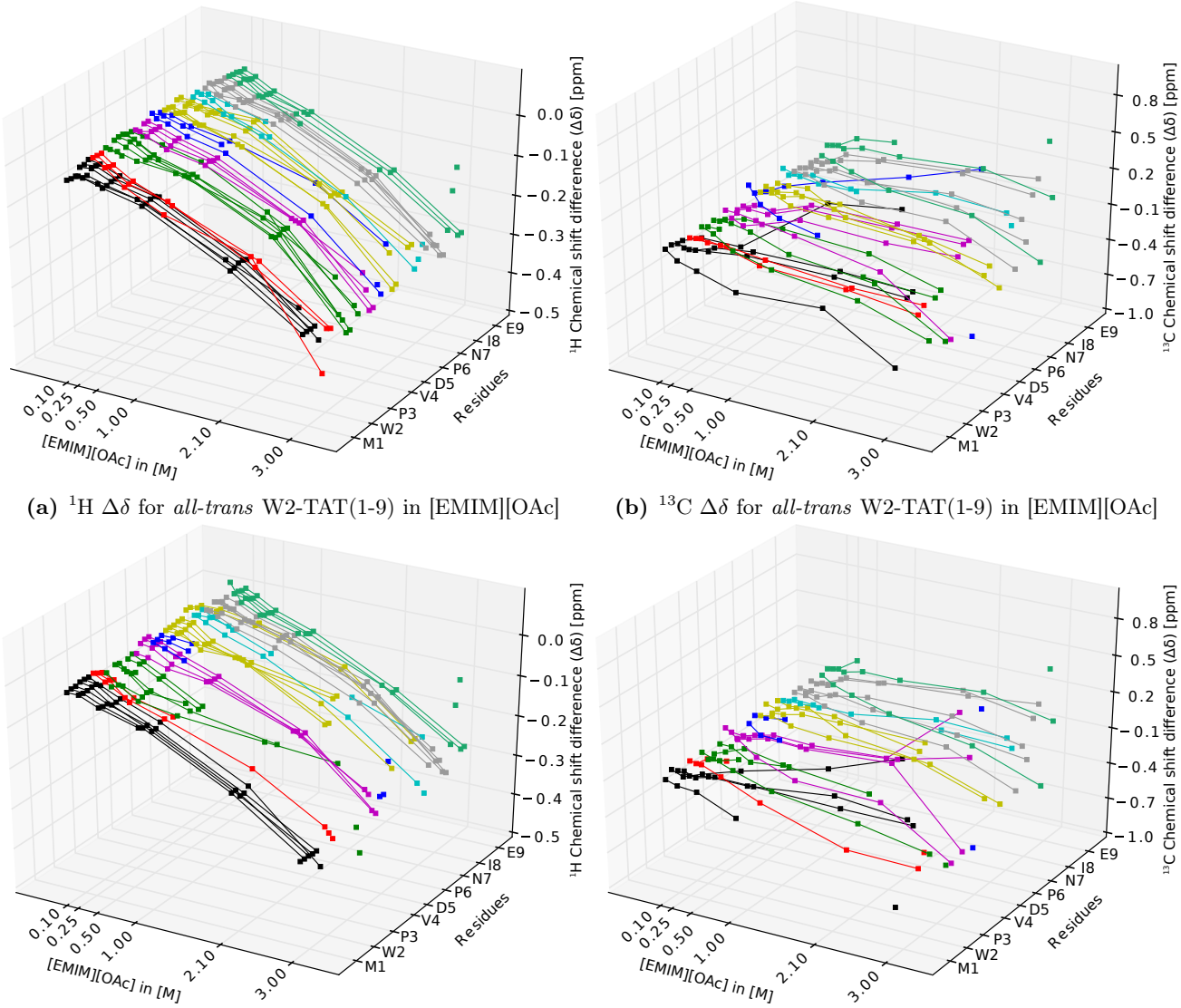

(a) ^{1}H $\Delta\delta$ for *all-trans* W2-TAT(1-9) in [EMIM][OAc]

(b) ^{13}C $\Delta\delta$ for *all-trans* W2-TAT(1-9) in [EMIM][OAc]

(c) ^{1}H $\Delta\delta$ for *cis* W2-TAT(1-9) in [EMIM][OAc]

(d) ^{13}C $\Delta\delta$ for *cis* W2-TAT(1-9) in [EMIM][OAc]

Fig. S 10: ^{1}H and ^{13}C chemical shift differences ($\Delta\delta$) of protons and carbons for *all-trans*- (upper panel) and *cis*-configured (lower panel) W2-TAT(1-9) as function of [EMIM][OAc] concentration. The reference system was 10 mM W2-TAT(1-9), pH 6.5, in 90/10% H_2O/D_2O. The peptide concentration was 10 mM for samples up to 2.1 M [EMIM][OAc] and experiments were carried out with a 5 mm room-temperature BBI-probe. Spectra for 3 M [EMIM][OAc] were carried out with a 4 mm triple resonance HR-MAS probe at 6 kHz spinning rate and a W2-TAT(1-9) concentration of 90 mM. All NMR experiments were acquired at 303 K and the pH was adjusted to 6.5. Depicted are all ^{1}H and ^{13}C $\Delta\delta$ in sequential order per residue as given in Fig. S5 and S6.

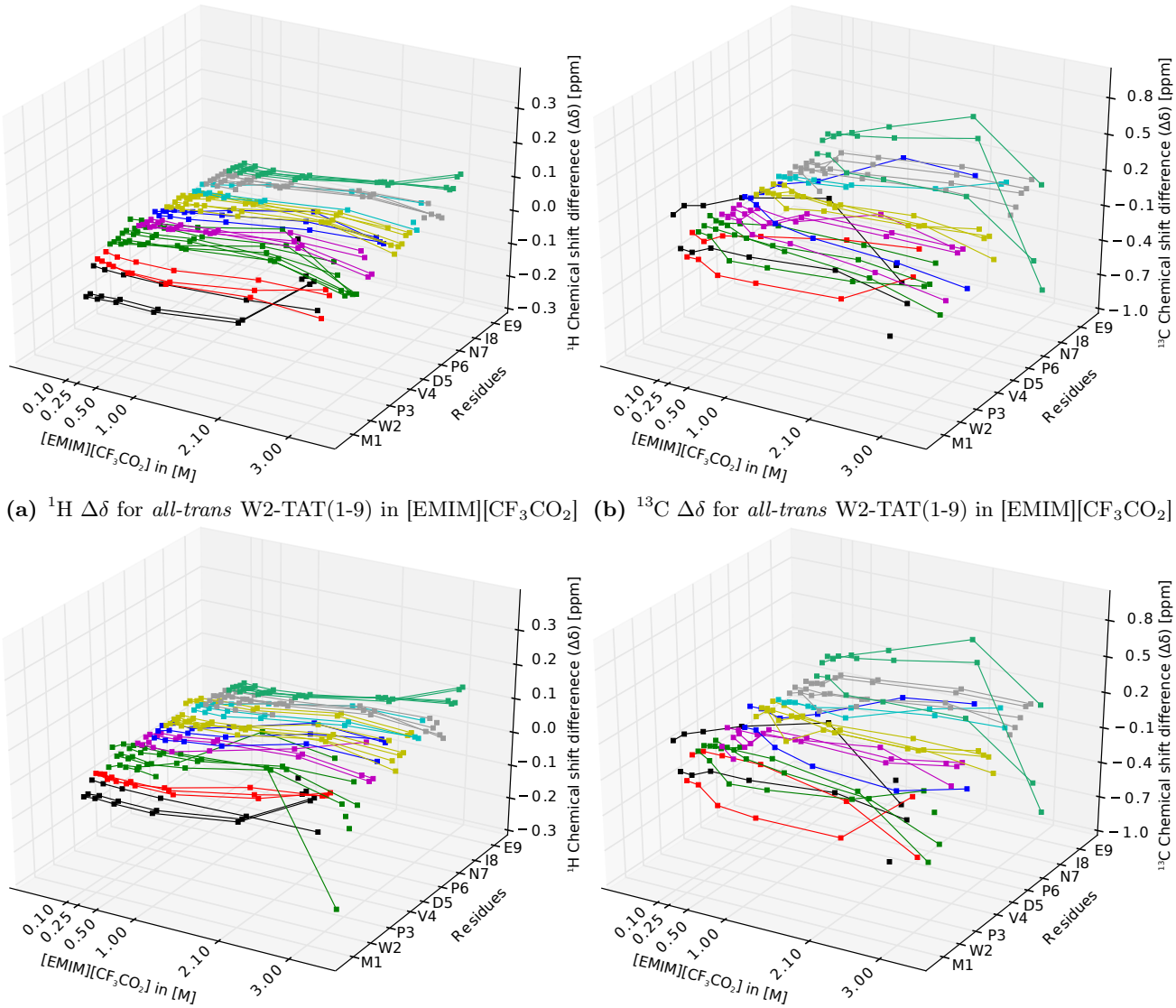

(a) ^{1}H $\Delta\delta$ for *all-trans* W2-TAT(1-9) in [EMIM][CF_3CO_2] **(b)** ^{13}C $\Delta\delta$ for *all-trans* W2-TAT(1-9) in [EMIM][CF_3CO_2]

(c) ^{1}H $\Delta\delta$ for *cis* W2-TAT(1-9) in [EMIM][CF_3CO_2] **(d)** ^{13}C $\Delta\delta$ for *cis* W2-TAT(1-9) in [EMIM][CF_3CO_2]

Fig. S 11: ^{1}H and ^{13}C chemical shift differences ($\Delta\delta$) of protons and carbons for *all-trans*- (upper panel) and *cis*-configured (lower panel) W2-TAT(1-9) as function of [EMIM][CF_3CO_2] concentration. The reference system was 10 mM W2-TAT(1-9), pH 6.5, in 90/10% H_2O/D_2O. The peptide concentration was 10 mM for samples up to 2.1 M [EMIM][CF_3CO_2] and experiments were carried out with a 5 mm room-temperature BBI-probe. Spectra for 3 M [EMIM][CF_3CO_2] were carried out with a 4 mm triple resonance HR-MAS probe at 6 kHz spinning rate and a W2-TAT(1-9) concentration of 90 mM. All NMR experiments were acquired at 303 K and the pH was adjusted to 6.5. Depicted are all ^{1}H and ^{13}C $\Delta\delta$ in sequential order per residue as given in Fig. S5 and S6.

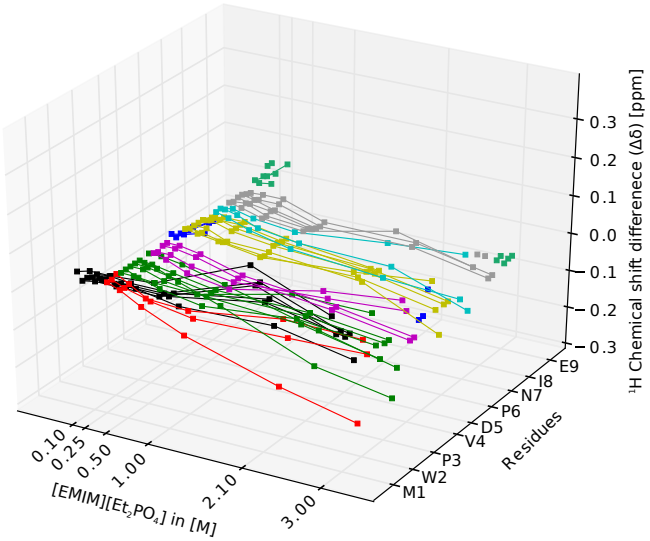

(a) ^{1}H $\Delta\delta$ for *all-trans* W2-TAT(1-9) in [EMIM][Et_2PO_4]

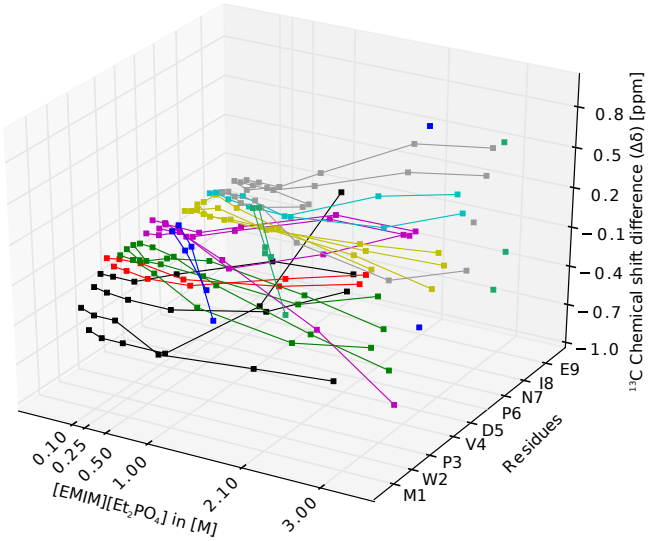

(b) ^{13}C $\Delta\delta$ for *all-trans* W2-TAT(1-9) in [EMIM][Et_2PO_4]

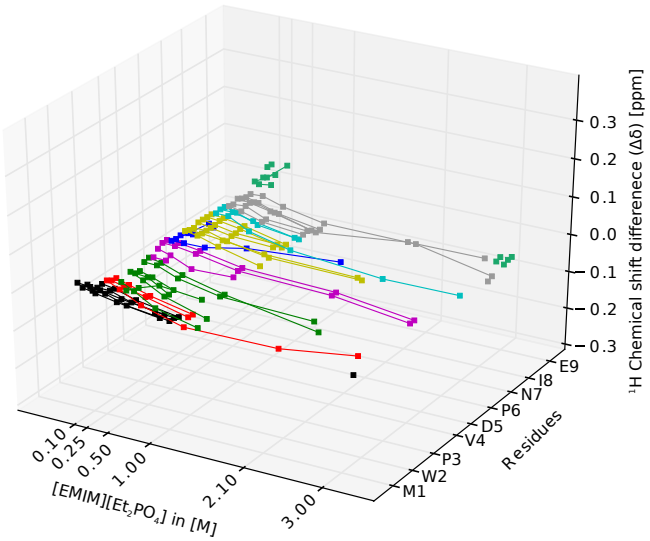

(c) ^{1}H $\Delta\delta$ for *cis* W2-TAT(1-9) in [EMIM][Et_2PO_4]

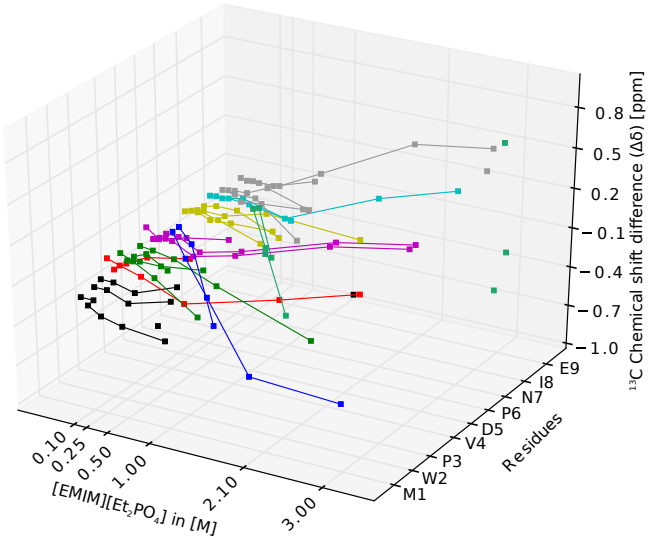

(d) ^{13}C $\Delta\delta$ for *cis* W2-TAT(1-9) in [EMIM][Et_2PO_4]

Fig. S 12: ^{1}H and ^{13}C chemical shift differences ($\Delta\delta$) of protons and carbons for *all-trans*- (upper panel) and *cis*-configured (lower panel) W2-TAT(1-9) as function of [EMIM][Et_2PO_4] concentration. The reference system was 10 mM W2-TAT(1-9), pH 6.5, in 90/10% H_2O/D_2O. The peptide concentration was 10 mM for samples up to 2.1 M [EMIM][Et_2PO_4] and experiments were carried out with a 5 mm room-temperature BBI-probe. Spectra for 3 M [EMIM][Et_2PO_4] were carried out with a 4 mm triple resonance HR-MAS probe at 6 kHz spinning rate and a W2-TAT(1-9) concentration of 90 mM. All NMR experiments were acquired at 303 K and the pH was adjusted to 6.5. Depicted are all ^{1}H and ^{13}C $\Delta\delta$ in sequential order per residue as given in Fig. S5 and S6.

Table S 4: Linear regression analysis of W2-TAT(1-9) ^{1}H and ^{13}C chemical shifts in different ILs as shown in Figure S9-12. The slope is given in $\Delta\delta$/M [ppm/M] IL.

	trans		*cis*	
	^{1}H	^{13}C	^{1}H	^{13}C
[EMIM][Br]	0.083±0.019	0.119±0.074	0.092±0.029	0.071±0.046
[EMIM][Et_2PO_4]	-0.024±0.034	-0.059±0.153	-0.047±0.037	-0.123±0.252
[EMIM][CF_3CO_2]	0.013±0.021	-0.001±0.083	0.010±0.041	-0.035±0.117
[EMIM][OAc]	-0.096± 0.019	-0.108±0.069	-0.067±0.035	-0.101±0.123

Table S 5: Effect of ILs and 0.5 M LiCl in TFE on the W2-TAT(1-9) *all-trans/cis* equilibrium state obtained by ^{1}H NMR spectroscopy. Presented are the *cis*-population contents. Conditions: 10 mM W2-TAT(1-9), pH adjusted to 6.5, were dissolved in the respective IL. The reference system was 10 mM W2-TAT(1-9), pH 6.5, in 90/10% H_2O/D_2O.

	IL concentration						
Solvent system	0 M	0.1 M	0.25 M	0.5 M	1 M	2.1 M	3 M
H_2O/D_2O	0.46						
TFE−d_3/ 0.5M LiCl	0.64						
[EMIM][OAc]	0.47	0.48	0.46	0.42	0.38	0.32	0.27
[MMIM][Me_2PO_4]	0.49	0.42	0.39	0.36	0.32	0.30	0.29
[EMIM][Me_2PO_4]	0.47	0.40	0.36	0.33	0.29	0.28	0.29
[EMIM][Et_2PO_4]	0.48	0.48	0.47	0.44	0.43	0.37	0.33
[EMIM][CF_3CO_2]	0.45	0.38	0.34	0.29	0.26	0.27	0.29
[EMIM][Cl]	0.47	0.45	0.42	0.39	0.37	0.35	0.31
[EMIM][Br]	0.47	0.39	0.36	0.35	0.31	0.35	0.30
[EMIM][SCN]	0.46	0.40	0.38	0.35	0.35	0.25	0.29

References Supplementary Data

[1] Christoph Wiedemann, Peter Bellstedt, and Matthias Görlach. Capito–a web server-based analysis and plotting tool for circular dichroism data. *Bioinformatics*, 29(14):1750–1757, Jul 2013.

[2] Vladimir N. Uversky. Natively unfolded proteins: a point where biology waits for physics. *Protein Sci*, 11(4):739–756, Apr 2002.

[3] N. Sreerama and R. W. Woody. Estimation of protein secondary structure from circular dichroism spectra: comparison of CONTIN, SELCON, and CDSSTR methods with an expanded reference set. *Anal Biochem*, 287(2):252–260, Dec 2000.

[4] W. Kabsch and C. Sander. Dictionary of protein secondary structure: pattern recognition of hydrogen-bonded and geometrical features. *Biopolymers*, 22(12):2577–2637, Dec 1983.

[5] Alfonso De Simone, Andrea Cavalli, Shang-Te Danny Hsu, Wim Vranken, and Michele Vendruscolo. Accurate random coil chemical shifts from an analysis of loop regions in native states of proteins. *J Am Chem Soc*, 131(45):16332–16333, Nov 2009.

[6] Mario Schubert, Dirk Labudde, Hartmut Oschkinat, and Peter Schmieder. A software tool for the prediction of Xaa-Pro peptide bond conformations in proteins based on 13C chemical shift statistics. *J Biomol NMR*, 24(2):149–154, Oct 2002.

[7] Yang Shen and Ad Bax. Prediction of Xaa-Pro peptide bond conformation from sequence and chemical shifts. *J Biomol NMR*, 46(3):199–204, Mar 2010.